

# Incommensurate magnetism in cuprate materials

F. Mancini and D. Villani

*Dipartimento di Scienze Fisiche "E. R. Caianiello" - Unità I.N.F.M. di Salerno  
Università di Salerno, 84081 Baronissi (SA), Italy*

H. Matsumoto

*Institute for Material Research, Tohoku University, Sendai 980, Japan  
(December 16, 1996)*

In the low doping region an incommensurate magnetic phase is observed in  $La_{2-x}Sr_xCuO_4$ . By means of the composite operator method we show that the single-band 2D Hubbard model describes the experimental situation. In the higher doping region, where experiments are not available, the incommensurability is depressed owing to the van Hove singularity near the Fermi level. A proportionality between the incommensurability amplitude and the critical temperature is predicted, suggesting a close relation between superconductivity and incommensurate magnetism.

PACS numbers: 74.72.-h, 75.10.-b, 71.10.Fd

The dynamical spin susceptibility for cuprate materials has been investigated by inelastic neutron scattering and NMR techniques. Neutron scattering data on  $La_{2-x}(Ba, Sr)_xCuO_4$  have shown [1-7] that away from half-filling the commensurate antiferromagnetic phase is suppressed and short-range incommensurate antiferromagnetism develops. The magnetic Bragg peak in the dynamical structure factor  $S(\mathbf{k}, \omega)$  broadens and develops a structure with four peaks located at  $[(1 \pm \delta)\pi, \pi]$  and  $[\pi, (1 \pm \delta)\pi]$ . The incommensurability amplitude  $\delta(x)$  does not depend on the frequency and temperature; it is zero up to the doping  $x \approx 0.05$  where a commensurate-incommensurate transition is observed, then, increases with the hole concentration  $x$ , following the linear law  $\delta(x) \approx 2x$  up to  $x \approx 0.12$ ; beyond this point there is a deviation downwards [7]. Unfortunately, experimental data above  $x = 0.18$  are not available, due to the difficulty in preparing single crystals. It is important to stress [5] that the value of doping  $x = 0.05$ , where the transition is observed, corresponds to the value of doping where the material becomes superconducting. These incommensurate spin fluctuations are not observed in other cuprate materials; a flat topped magnetic peak has been observed [8] in  $YBa_2Cu_3O_{6+y}$  with  $y \approx 0.6$ , while for the case of the electron-doped  $Nd_{2-x}Ce_xCuO_4$  no incommensurate magnetism has been observed [9]. The difference in the spatial modulation experimentally observed in  $La_{2-x}Sr_xCuO_4$  and  $YBa_2Cu_3O_{6+y}$  has been related to a difference in the topology of the Fermi surface [10,11].

From a theoretical side the presence of incommensurate magnetic correlations was firstly found in the 2D Hubbard [12] and in the  $t - J$  model [13] by Quantum Monte Carlo (QMC) calculations. To improve the situation the  $t - t'$  Hubbard model has been considered, but the results are not definite and there is no general agreement [14].

In this Letter we shall study the spin magnetic sus-

ceptibility of the two-dimensional single-band Hubbard model by means of the Composite Operator Method (COM) [15-16]. We have shown [16] that in the static approximation the dynamical spin susceptibility is given by the following expression:

$$\chi(\mathbf{k}, \omega) = \frac{2}{n^2 - n - 2D} [n (Q_{1111}^R + 2Q_{1112}^R + Q_{1212}^R) + (2 - n) (Q_{1212}^R + 2Q_{1222}^R + Q_{2222}^R)] \quad (1)$$

where  $n$  is the particle density,  $D$  is the double occupancy and by  $Q_{\alpha\beta\gamma\delta}^R(\mathbf{k}, \omega)$  we mean the retarded part of  $Q_{\alpha\beta\gamma\delta}(\mathbf{k}, \omega) = i \int \frac{d^2p d\Omega}{(2\pi)^3} G_{\alpha\beta}(\mathbf{k} + \mathbf{p}, \omega + \Omega) G_{\gamma\delta}(\mathbf{p}, \Omega)$ . The  $2 \times 2$  matrix  $G(\mathbf{k}, \omega)$  is the thermal causal Green's function, defined by  $G(\mathbf{k}, \omega) = \langle T[\psi(i)\psi^\dagger(j)] \rangle_{F.T.}$ , where  $\psi(i)$  is the doublet composite operator

$$\psi(i) = \begin{pmatrix} \xi(i) \\ \eta(i) \end{pmatrix} \quad (2)$$

with  $\xi_\sigma(i) = c_\sigma(i) [1 - n_{-\sigma}(i)]$  and  $\eta_\sigma(i) = c_\sigma(i) n_{-\sigma}(i)$ .  $c_\sigma(i)$  is the electron operator at site  $i$ . By means of the equation of motion and by considering the static approximation, where finite lifetime effects are neglected, the Green's function  $G(\mathbf{k}, \omega)$  can be computed in the course of a fully self-consistent calculation where no adjustable parameters are considered [15].

The calculation of the uniform static susceptibility  $\chi_0(x, T)$  for various values of doping and temperature has been given in Ref. 16, where we showed that Eq. (1) qualitatively reproduces the experimental situation observed in  $La_{2-x}Sr_xCuO_4$ . The principal results obtained in Ref. 16 can be so summarized. For a fixed temperature,  $\chi_0(x, T)$  is an increasing function of the doping, reaches a maximum at a critical doping  $x_c$ , then decreases. The value of  $x_c$  does not change with temperature and is determined by the ratio  $U/t$ , varying from 0 to  $1/3$  when  $U/t$  changes from zero to infinite; for  $U/t = 4$

we have  $x_c = 0.27$ . This doping dependence qualitatively reproduces the experimental behavior observed in  $La_{2-x}Sr_xCuO_4$  [17], where a critical value  $x_c \approx 0.25$  is reported. For a given doping, when the system is away from the critical density,  $\chi_0(x, T)$  as a function of temperature has a behavior similar to a 2D Heisenberg antiferromagnet with a maximum at a certain temperature  $T_m$ ; the position of  $T_m$  decreases as the system is doped away from half-filling and tends to zero for  $x \rightarrow x_c$ ; in the vicinity of the critical doping there is a large increase of  $\chi_0(x, T)$  for low temperatures. The behaviors of  $T_m$  as a function of  $x$  and of  $\chi_0(x, T)$  as a function of  $T_m$  well reproduce the experimental data of Ref. 17.

The peak exhibited by  $\chi_0(x, T)$  for a certain critical doping is related to the fact that for  $x = x_c$  the Fermi energy crosses the vHs. This can be seen in Fig. 1, where  $N(E_F)$ , the density of states calculated at the Fermi energy, and  $\chi_0(x, T)$ , the uniform static susceptibility, are given versus the doping parameter  $x$ . We have chosen  $U/t = 4$  and  $k_B T/t = 0.01$ . At half-filling the Fermi energy is at the center of the two Hubbard bands; by varying the dopant concentration some weight is transferred from the upper to the lower band,  $E_F$  moves to lower energies and crosses the vHs for a critical value of the doping; further increasing  $x$ ,  $E_F$  moves away from the vHs. A study of the Fermi surface shows that for  $x > x_c$  we have a closed surface which becomes nested at  $x = x_c$  and opens for  $x < x_c$ . An enlarged Fermi surface with a volume larger than the noninteracting one has been reported by QMC calculations [18,19] and by other theoretical works [20].

To understand the role played by the vHs in the case of spin fluctuations, it is useful at first to consider the case of noninteracting Hubbard model (i.e.  $U = 0$ ). What we learn [21] from the study of this model can be so summarized.

- The  $\mathbf{k}$ -dependent susceptibility  $\chi(\mathbf{k})$  exhibits a maximum at a certain value  $\mathbf{k}^*$  which depends on the position of the vH energy  $\omega_{vH}$  with respect to the Fermi energy  $E_F$ .
- When  $n = 1$   $\omega_{vH} = E_F$  and  $\mathbf{k}^* = \mathbf{Q} = (\pi, \pi)$ . In addition there is a singularity coming from the nesting of the Fermi surface and the staggered susceptibility  $\chi(\mathbf{Q})$  exhibits a stronger divergence than  $\chi_0$ .
- When  $n \neq 1$  the Bragg peak at  $\mathbf{Q} = (\pi, \pi)$  opens in four peaks, situated at  $\mathbf{k}^* = [\pi(1 \pm \delta), \pi(1 \pm \delta)]$ ; there is a transition from commensurate to incommensurate magnetism. The incommensurability amplitude  $\delta(x)$  increases as a function of the doping  $x$  with the same law as the shifting of  $E_F$  with respect to the vHs:

$$\begin{aligned} \omega_{vH} - E_F &\approx ax^{4/3} & a &\approx 3.62 \\ \delta(x) &\approx bx^{4/3} & b &\approx 1.31 \end{aligned} \quad (3)$$

In the interacting case, the shifting of the vHs and the band structure have a drastic influence on the form of

the susceptibility. Calculations based on the use of Eq. (1) show that around  $\mathbf{Q} = (\pi, \pi)$   $\chi(\mathbf{k})$  has an incommensurate structure along the four corners of a square, with a minimum at  $\mathbf{Q}$ . This incommensurate structure contains a mixing of two components. The relative position and the intensity of the two contributions change significantly with doping. To study the effect of the interaction we see that the  $k$ -dependent susceptibility  $\chi(\mathbf{k})$  can be written as  $\chi(\mathbf{k}) = \sum_{i,j=1}^2 \chi_{ij}(\mathbf{k})$  where

$$\chi_{ij}(\mathbf{k}) = \int \frac{d^2 p}{(2\pi)^2} \frac{f[E_i(\mathbf{k} + \mathbf{p})] - f[E_j(\mathbf{p})]}{E_i(\mathbf{k} + \mathbf{p}) - E_j(\mathbf{p})} K_{ij}(\mathbf{k}, \mathbf{p}) \quad (4)$$

The quantities  $K_{ij}(\mathbf{k}, \mathbf{p})$  are expressed in terms of the spectral intensities. The term  $\chi_{inter} = \chi_{12} + \chi_{21}$  describes transitions between the two bands  $E_1(\mathbf{k})$ , the upper Hubbard band, and  $E_2(\mathbf{k})$ , the lower Hubbard band; while the two terms  $\chi_{11}$  and  $\chi_{22}$  describe intraband transitions. Since  $E_1$  takes values mostly above the chemical potential, the contribution of  $\chi_{11}$  is small. The interband term  $\chi_{inter}$  is reported in Fig. 2. This term originates a peak in the susceptibility, which moves from the commensurate position  $\mathbf{Q} = (\pi, \pi)$  to  $(\pi, \pi/2)$  when the doping is increased from  $x = 0$  to  $x = x_c$ . The intensity of the peak decreases by increasing doping. The intraband term  $\chi_{22}$  is reported in Fig. 3. This term gives a peak which is a reminiscent of the Van Hove singularity in the density of states. At zero doping the vHs is far from the Fermi energy and the peak is located  $(\pi/\pi/2)$  and has a low intensity. When doping increases, the peak increases its intensity and moves along the line  $(k_x = \pi, \pi/2 \leq k_y < 3\pi/2)$ . At the critical doping  $x = x_c$  the vHs lies on the Fermi energy and the Fermi surface is nested. Then, the peak of  $\chi_{22}$  is situated at  $\mathbf{Q}$  and has a very high intensity, due to the concomitance of these two effects. It is interesting to note that the peak position of  $\chi_{22}$  moves towards  $\mathbf{Q}$  with the same law as given in Eq. 3.

The total susceptibility is reported in Fig. 4 for three values of doping. For zero doping we mainly have a commensurate structure with a peak coming from  $\chi_{inter}$ , located at  $(\pi, \pi)$ , and a smaller peak, coming from  $\chi_{22}$ , located near  $(\pi, \pi/2)$ . Upon doping, the two peaks moves for different reasons.  $\chi_{22}$  moves because the Van Hove singularity moves towards the Fermi energy.  $\chi_{inter}$  moves because the band structure changes with doping. When the critical doping  $x = x_c$  is reached, the Van Hove singularity is at the Fermi energy and the Fermi surface is nested. A commensurate structure is recovered with a very high peak coming from  $\chi_{22}$ .

In Fig. 5 the incommensurability amplitude  $\delta(x)$  is reported as a function of doping. In the region of low (high) doping the peak coming from  $\chi_{inter}$  ( $\chi_{22}$ ) is predominant and very well separated from the other; in these regions  $\delta(x)$  has been evaluated as the middle point of the half-width of the peak. In the region  $0.10 \leq x \leq 0.18$  the two peaks overlap and  $\delta(x)$  has been calculated by taking the

average of both peaks and we have a plateau due to the superimposition of  $\chi_{22}$  and  $\chi_{inter}$ . For comparison we report the experimental data of Refs. 4, 5 and 7. The linear behavior of  $\delta(x)$ , observed in the low doping region, agrees exceptionally well with the experimental data, reported in Refs. 4-7; the downward deviation reported in Ref. 7 for  $x > 0.12$  might correspond to the plateau theoretically observed. One of the most striking feature of the results presented in Fig. 5 is the similarity between the incommensurability amplitude  $\delta(x)$  and the critical temperature  $T_c$ .  $\delta(x)$  is maximum in the region of optimal doping where  $T_c$  is maximum. It has already been observed in Ref. 7 that there is a linear relation between  $\delta(x)$  and  $T_c$  up to the optimal doping level  $x \simeq 0.15$ . Our theoretical results extend to the all region of doping a relation of proportionality between  $\delta(x)$  and  $T_c$ .

The same result for  $\delta(x)$  can be obtained by considering  $\text{Im } \chi(\mathbf{k}, \omega)$ . Some results have been given in Ref. 22. We preferred to study the  $\mathbf{k}$ -dependent susceptibility  $\chi(\mathbf{k})$  because this quantity provides more strict information about the spatial range of the magnetic correlations. On the other hand an exact experimental determination of  $\chi(\mathbf{k})$  is not easy, since it must be calculated by the accessible  $S(\mathbf{k}, \omega)$  through a Kramers-Kronig relation.

The present analysis shows that the interaction in the Hubbard model has mainly two effects. One is the change of the critical doping from  $x = 0$  to some critical  $x_c$ , due to the shift of the vHs. This shift explains and well reproduces the unusual normal state behavior of  $\chi_0$  in hole-doped cuprates. The other is a band structure effect which is responsible of the incommensurate modulation of the magnetic susceptibility in the low doping region.

The picture that emerges is that the magnetism probed by neutron scattering experiments is correlated with the carrier density. In the low doping region the susceptibility is mainly controlled by the term  $\chi_{inter}$  which describes band structure effects and then reflects the topology of the Fermi surface. In the overdoped region the Fermi energy is close to the vHs and the effect of nesting in the intraband term is important. In  $YBa_2Cu_3O_{6+y}$  we have a different topology of the Fermi surface and no nesting is expected; this might be the reason why incommensurability is not observed.

The main results obtained in this Letter can be so summarized. There is experimental evidence that in hole-doped high  $T_c$  cuprates the Fermi level is close to the vHs for values of doping close to those where the superconducting phase is suppressed. In the context of the Hubbard model a van Hove scenario well describes some of the unusual properties observed in the normal state, but an analysis show that this scenario is related to the overdoped region and not to the optimal doping. The existence of a critical doping where the vHs lies on the Fermi energy should imply a peak in the staggered susceptibility. Then, we predict that commensurate magnetism should be recovered

in the nearness of the critical doping, implying a proportionality relation between the incommensurability amplitude  $\delta(x)$  and the superconducting critical temperature. Recalling that in  $La_{2-x}Sr_xCuO_4$  the commensurate-incommensurate transition is observed at the same value of doping  $x \simeq 0.05$  where superconductivity starts, at least for  $La_{2-x}Sr_xCuO_4$ , a scenario [23] which relates the superconducting phase to the presence of incommensurate magnetism emerges.

## ACKNOWLEDGMENTS

The authors wish to thank Prof. M. Marinaro and Dr. A. Avella for many valuable discussions.

- 
- [1] T.R. Thurston et al., Phys. Rev. B **40**, 4585 (1989).
  - [2] G. Shirane et al., Phys. Rev. Lett. **63**, 330 (1989).
  - [3] R.J. Birgeneau et al., Phys. Rev. B **38**, 6614 (1988).
  - [4] S.W. Cheong et al., Phys. Rev. Lett. **67**, 1791 (1991).
  - [5] G. Shirane, R.J. Birgeneau, Y. Endoh and M.A. Kastner, Physica B **197**, 158 (1994).
  - [6] K. Yamada et al., Phys. Rev. Lett. **75**, 1626 (1995).
  - [7] K. Yamada et al., "Doping dependence of the spatially modulated dynamical spin correlations and the superconducting transition temperature in  $La_{2-x}Sr_xCuO_4$ ", Preprint 1996.
  - [8] M. Tranquada et al., Phys. Rev. B **46**, 5561 (1992).
  - [9] T.R. Thurston et al., Phys. Rev. Lett. **65**, 263 (1990).
  - [10] J. Rossat-Mignod et al., Physica B **169**, 58 (1991).
  - [11] R. Liu et al., Phys. Rev. B **46**, 11056 (1992).
  - [12] A. Moreo et al, Phys. Rev. B **41**, 2313 (1990).
  - [13] A. Moreo, E. Dagotto, T. Jolicoeur and J. Riera, Phys. Rev. B **42**, 6283 (1990).
  - [14] P. Bénard, L. Chen and A.M. Tremblay, Phys. Rev. B **47**, 15217 (1993); *ibid* **47**, 589 (1993); Q. Si, T. Zha, K. Levin and J.P. Lu, Phys. Rev. B **47**, 9055 (1993); N. Furukawa and M. Imada, J. Phys. Soc. Jpn. **61**, 3331 (1992); R.J. Gooding, K.J.E. Vos and P.W. Leung, Phys. Rev. B **49**, 4119 (1994); *ibid* **50**, 12866 (1994).
  - [15] F. Mancini, S. Marra and H. Matsumoto, Physica C **244**, 49 (1995); *ibid* **250**, 184 (1995).
  - [16] F. Mancini, S. Marra and H. Matsumoto, Physica C **252**, 361 (1995).
  - [17] J.B. Torrance et al. Phys. Rev. B **40**, 8872 (1989).
  - [18] N. Bulut, D.J. Scalapino and S.R. White, Phys. Rev. B **50**, 7215 (1994); N. Bulut, D.J. Scalapino and S.R. White, Phys. Rev. Lett. **73**, 748 (1994).
  - [19] D. Duffy and A. Moreo, Phys. Rev. B **52**, 15607 (1995).
  - [20] D.M. Newns, P.C. Pattnaik and C.C. Tsuei, Phys. Rev. B **43**, 3075 (1991); J. Beenen and D.M. Edwards, Phys. Rev. B **52**, 13636 (1995).
  - [21] F. Mancini, D. Villani and H. Matsumoto, to be published.

- [22] F. Mancini, H. Matsumoto and D. Villani, Czechoslovak Journ. of Physics, **46** suppl. S4, 1871 (1996).
- [23] F. Mancini, S. Marra and H. Matsumoto, Physica C **263**, 70 (1996); F. Mancini, V. Oudovenko and D. Villani, Czechoslovak Journ. of Physics, **46** suppl. S4, 1873 (1996).

### Figure Captions

Fig. 1 The density of states at the Fermi energy  $N(E_F)$  and the uniform static susceptibility  $\chi_0(x, t)$  as functions of the doping  $x$ .  $U/t = 4$  and  $k_B T/t = 0.01$ .

Fig. 2 The interband term  $\chi_3(\mathbf{k})$  along the line  $\mathbf{k} = (\pi, k_y)$  for  $k_B T/t = 0.01$  and for various values of the doping  $x \leq 0.27$  with step 0.03.  $U/t = 4$ .

Fig. 3 The intraband term  $\chi_2(\mathbf{k})$  along the line  $\mathbf{k} = (\pi, k_y)$  for  $k_B T/t = 0.01$  and for various values of the doping  $x \leq 0.27$  with step 0.03.  $U/t = 4$ .

Fig. 4 The spin magnetic susceptibility  $\chi(\mathbf{k})$  along the line  $\mathbf{k} = (\pi, k_y)$  for various values of the doping  $x$ .  $U/t = 4$  and  $k_B T/t = 0.01$ .

Fig. 5 The incommensurability amplitude  $\delta(x)$  as a function of the doping  $x$ . The dashed line indicates the theoretical result.  $U/t = 4$  and  $k_B T/t = 0.01$ .

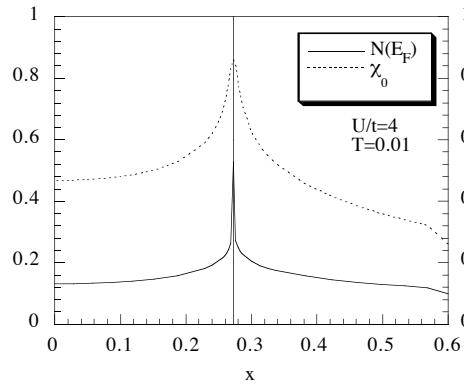


Fig. 1

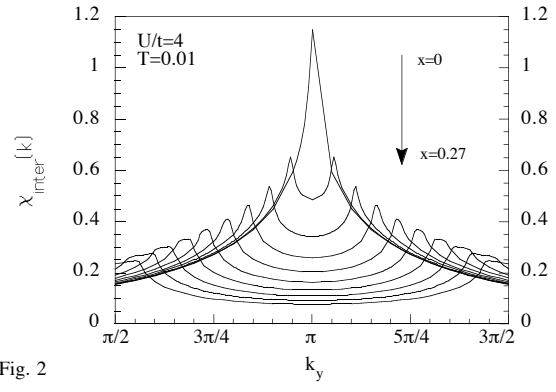


Fig. 2

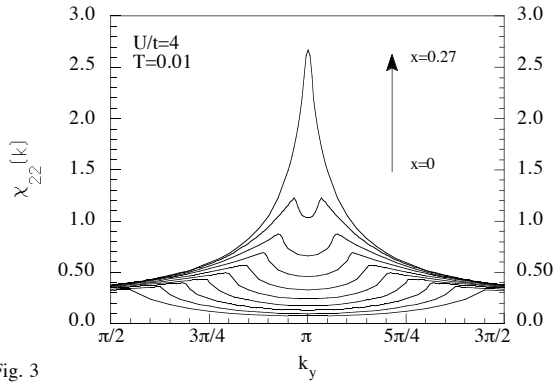


Fig. 3

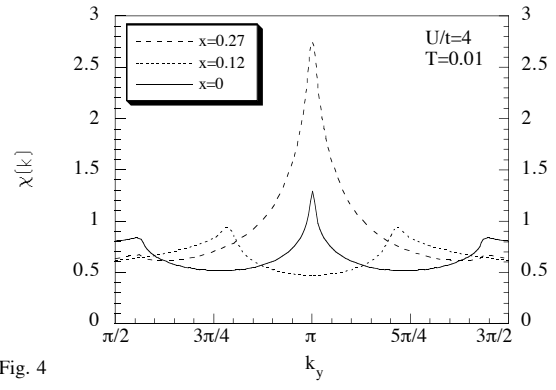


Fig. 4

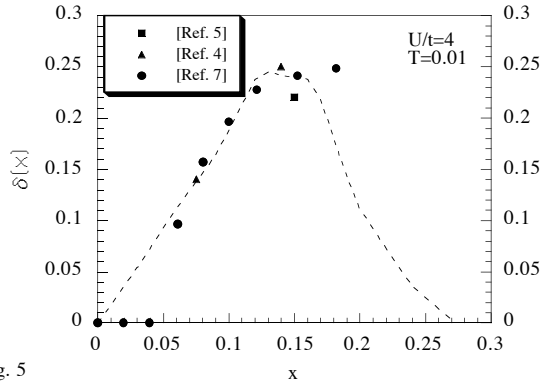


Fig. 5